TECHNICAL REPORT

ESA contract No. AO/1-10968/22/NL/MG	Company: Maana Electric SA	
SUBJECT: DIESAMP EXECUTIVE SUMMARY REPORT		
Date: 30/01/2025	No. of volumes: 1 This is volume: 1	Contractor's reference: Luca Celiento

ABSTRACT: This report summarizes the results of the ESA activity "Development and Integration of Embedded Sensors for Advanced Manufacturing Processes" (DIESAMP), conducted under contract AO/1-10968/22/NL/MG. The project integrates embedded sensors — such as temperature and strain sensors — into a novel Deployable Solar Array concept, aligning with ESA's Advanced Manufacturing Initiative to improve space product's performance, reduce costs, and enable real-time data acquisition. Using additive manufacturing techniques inkjet-printed sensors have been embedded into a Deployable Solar Array, achieving Technology Readiness Level (TRL) 4. Breadboards were developed and tested in relevant conditions. A roadmap for further development is presented, targeting future applications in satellite operations and lunar exploration while addressing challenges in manufacturing and system resilience.

The work described in this report was done by Maana Electric's employee(s) and its partners. The property of the contents resides in Maana Electric only and consortium represented. The information contained in this document is confidential and no one else is authorized to distribute, forward, print, copy or act upon any information contained.

Authors:
Luca Celiento

ESA study manager: Division: Directorate:	ESA budget heading: Division: Directorate:

© MAANA ELECTRIC S.A. [2024]

The copyright in this document is vested in MAANA ELECTRIC S.A.

This document may only be reproduced in whole or in part, or stored in a retrieval system, or transmitted in any form, or by any means electronic, mechanical, photocopying or otherwise, either with the prior permission of MAANA ELECTRIC S.A. or in accordance with the terms of ESA Contract No. AO/1-10968/22/NL/MG.

Table of Contents

1 Introduction 1
2 References 1
  2.1 Applicable documents 1
  2.2 Reference documents 1
  2.3 Acronyms and abbreviations 1
3 Background and aim of the study 2
4 Key findings 2
  4.1 Product selection 2
  4.2 Sensors selection 4
  4.3 Deployable Solar Array (DSA) design 5
  4.4 Sensors manufacturing 7
  4.5 Breadboards 8
    4.5.1 DSA-PV 9
    4.5.2 DSA-M 14
5 Conclusions and future developments 21

List of Tables

Table 1. List of applicable documents. 1
Table 2. List of reference documents. 1
Table 3. List of acronyms and abbreviations. 1
Table 4. Results of the trade-off study for the selection of the space product to be adopted within this activity. 3
Table 5. Results of the trade-off study for the selection of the sensors to be embedded into the space product adopted within this activity. 4
Table 6. Summary of the results of TVAC testing on the DSA-PV breadboard. 13
Table 7. Summary of the results of deployment testing on the DSA-M breadboard. 17
Table 8. Summary of the results of deployment testing on the DSA-M breadboard....20

List of Figures

Figure 1. List of products identified by the application survey....... 3
Figure 2. A DSA in its deployed configuration and summary of its specifications. 5
Figure 3. Left: a DSA with lateral rows folded on the central one. Right: highlight of the segmented structure of the DSA, where each pair of PV cells forms a rigid segment connected to other segments by FPC. 5
Figure 4. Diagram showing the position of the strain and temperature sensors on one segment of the DSA....... 6
Figure 5. Left: the rear-side view of the deployed DSA, showing the deployable mechanism with proposed inflatable branching of the inflatable tubes. Right: highlight of the interface with the gas-management system and the physical holder of the Kapton® substrate....... 6
Figure 8. Process steps of sensors' inkjet printing proposed by LIST....... 7
Figure 6. Top and side-view of the flexible PCB design for integration of printed sensors....... 7
Figure 7. Proposed process flow for the manufacturing and integration of printed sensors into the DSA breadboards: 1) Printing of the gauge and the pads. 2) Spray-coating of an encapsulant. 3) Gluing sensors onto the flexible PCB. 4) Application of Ag epoxy....... 8
Figure 9. Final design of strain gauges and temperature sensors. 8
Figure 10. Left: CAD representation of the DSA-PV. Right: Stack structure of the FPC layers for the DSA breadboards....... 9
Figure 11. Right: CAD of the folded DSA-PV. Left: Highlight of the connection bridges when the segments were folded (top) and in the deployed configuration (bottom)... 10
Figure 13. Electrical and data design of DSA-PV's FPC. The top layer of the embedded circuits embedded in the PCB is on top of the Figure and highlights the circular pads for rear-connection of the first cells of a segment, the small square pads for connection of tab-wires of the second cells of a segment and finally the electrical connection between electrical interface and first segment, as well as electrical connections between segments. The bottom of the Figures shows the embedded circuits on the bottom layer of the FPC, which includes the electrical connection between the last segment and the interface (return electrical line), as well as the four sockets for the sensors and their data connections to the data interface. 11
Figure 13. TVAC set-up with the DSA-PV demonstrator. a) The demonstrator integrated on a thermal plate. b) Thermal filler (Sigraflex® graphize foil) which was placed between the two thermal plates. c) Flange with the KF50 feedthrough. d) The demonstrator integrated on thermal plate with attached thermocouples. e) The whole set-up is covered with MLI. 12
Figure 14. Response of the sensors integrated on the DSA-PV during TVAC cycling experiment....... 12
Figure 15. Visual appearance of the DSA-PV demonstrator before and after TVAC tests. 13
Figure 18. CAD representation of the DSA-M....... 14

Figure 17. Electrical and data design of DSA-PV's FPC. The top and bottom layers of the FPC are shown at top of the Figure. Details of the circuits in the two overlapping layers of the first two segments are shown at the bottom of the Figure. 15
Figure 18. Bottom view of the DSA-M in deployed configuration, showing the inflated tubes and their interfaces with the FPCs and the gas system. 16
Figure 21. Setup of deployment test: the DSA-M mounted in stowed configuration (top-left), a highlight of the data interface of the DSA-M (bottom-left), the DSA-M released from stowed configuration (top-right) and the DSA-M deployed with inflation. 16
Figure 20. Strain sensors reading during deployment test. Different colors denote different stages of deployment: "pressed", "released" and "inflated". 17
Figure 21. Setup of x-axis vibratory test of DSA-M. Left: the mechanical interface. Center: the DSA-M mounted. Right: the accelerometer. 18
Figure 22. Readings of the strain sensors (top) and temperature sensors (bottom) during random vibrations test on the x-axis. Grey area highlights the time of interest for the shaker test. 19
Figure 23. Readings of the strain sensors (top) and temperature sensors (bottom) during random vibrations test on the y-axis. Grey area highlights the time of interest for the shaker test. 19
Figure 24. Readings of the strain sensors (top) and temperature sensors (bottom) during random vibrations test on the z-axis. Grey area highlights the time of interest for the shaker test. 20

1 Introduction

The present document summarizes the key results and findings of the project "DIESAMP", providing a brief overview of the whole program, major findings, conclusions and further study areas.

2 References

2.1 Applicable documents

Table 1. List of applicable documents.

ID #	Title	Doc. No.
AD01		

2.2 Reference documents

Table 2. List of reference documents.

ID #	Title
RD-01	ESA-TECMS-TN-015895, Iss. 1, Rev. 0, 2019, Advanced Manufacturing for Space.
RD-02	ECSS-E-ST-10-04C Rev.1, Space environment (15 June 2020).
RD-03	ECSS-E-HB-11A, Technology readiness level (TRL) guidelines (1 March 2017).
RD-04	ECSS-E-ST-10-06C. Technical requirements specification (6 March 2009).

2.3 Acronyms and abbreviations

Table 3. List of acronyms and abbreviations.

Abbreviation	Meaning
AD	Applicable Document
AM	Advanced Manufacturing
BB	Breadboard
CAD	Computer Assisted Design
CFRP	Carbon Fiber Reinforced Polymer
COTS	Commercial Off-The-Shelf
DSA	Deployable Solar Array
FBG	Fiber Bragg Grating
FPC	Flexible Printed Circuit
IJP	InkJet Printing
LIST	Luxembourg Institute of Science and Technology
MLI	Multi-Layer Insulation
PCB	Printed Circuit Board

RD	Reference Document
RTD	Resistance Temperature Detector
TRL	Technology Readiness Level
TVAC	Thermal Vacuum

3 Background and aim of the study

This document serves as the Final Report for the ESA activity “DEVELOPMENT AND INTEGRATION OF EMBEDDED SENSORS FOR ADVANCED MANUFACTURING PROCESSES” (DIESAMP) under contract AO/1-10968/22/NL/MG. The activity aligns with ESA’s Advanced Manufacturing (AM) Cross-Cutting Initiative to enhance European space industry capabilities through smart manufacturing.

By embedding sensors such as temperature, pressure, and strain directly into spacecraft components, this initiative improves design flexibility, system performance, and cost efficiency while enabling real-time data collection throughout the product lifecycle.

In collaboration with LIST and Maana Electric, the project identified suitable space products and sensor technologies through a literature review and trade-off analysis, addressing challenges like durability in harsh environments and integration feasibility. The study focused on inkjet-printed thermal and strain sensors for a Deployable Solar Array, selected via systematic evaluation. Additive manufacturing techniques were adapted for sensor embedding, and breadboards were tested under relevant conditions to reach TRL 4 within the ESA GSTP framework. Finally a roadmap was established to guide further technology maturation and explore future space applications.

4 Key findings

4.1 Product selection

As a starting point for this activity, we have defined a list of components and critical applications of space systems where sensors can be embedded to. Different classes of sensors are required to be integrated with and within the system to provide and monitor seamless information about its health during various phases of the project like manufacturing, integration, testing, launching and service lifetime. The type and class of sensors are used based on space application and its mission statement whereby monitoring the health of the product during its lifecycle and collecting the lifecycle data. The following products have been identified in the frame of an application survey:

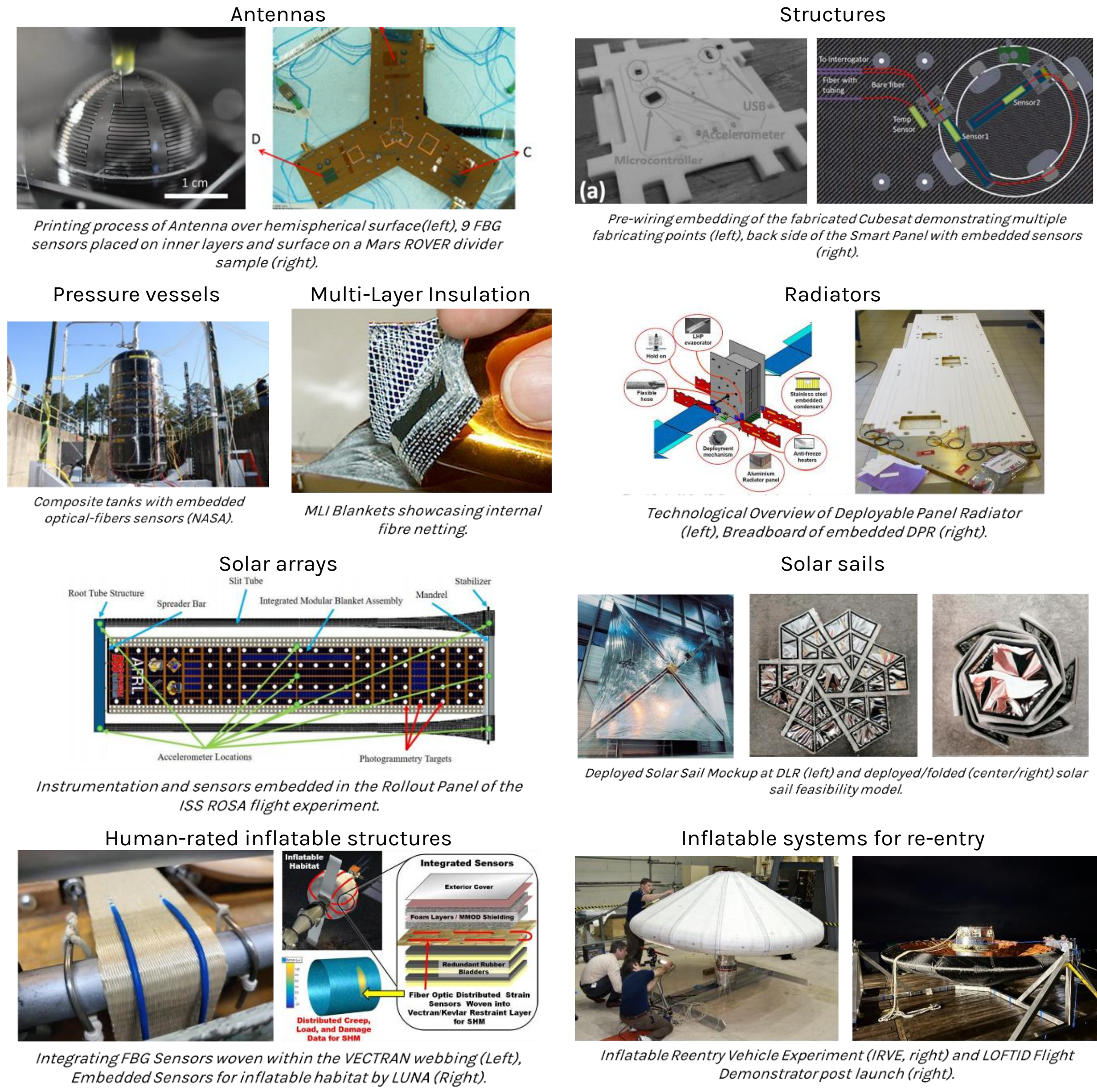

Printing process of Antenna over hemispherical surface(left), 9 FBG sensors placed on inner layers and surface on a Mars ROVER divider sample (right).

Pre-wiring embedding of the fabricated Cubesat demonstrating multiple fabricating points (left), back side of the Smart Panel with embedded sensors (right).

Composite tanks with embedded optical-fibers sensors (NASA).

MLI Blankets showcasing internal fibre netting.

Technological Overview of Deployable Panel Radiator (left), Breadboard of embedded DPR (right).

Instrumentation and sensors embedded in the Rollout Panel of the ISS ROSA flight experiment.

Deployed Solar Sail Mockup at DLR (left) and deployed/folded (center/right) solar sail feasibility model.

Integrating FBG Sensors woven within the VECTRAN webbing (Left), Embedded Sensors for inflatable habitat by LUNA (Right).

Inflatable Reentry Vehicle Experiment (IRVE, right) and LOFTID Flight Demonstrator post launch (right).

Figure 1. List of products identified by the application survey.

To determine which of identified candidates were best suited for embedding sensors, a trade study was performed. The results of the trade-off are presented as follows:

Table 4. Results of the trade-off study for the selection of the space product to be adopted within this activity.

Candidate	Life cycle	Technological benefit	Economic benefit	Manufacturing adaptability	Manufacturing complexity	Cost	Score
Antenna	F	F	MG	MP	F	MP	0.51
Composite Structure	MG	G	F	F	F	F	0.67
Pressure vessels/tanks	F	MG	F	MP	MP	F	0.52
Multi-layer insulation	MG	F	MG	MG	MP	MG	0.66
Radiators	F	F	F	F	F	MG	0.56

Deployable solar array	**MG**	**MG**	**MG**	**MG**	**F**	**MG**	**0.81**
Deployable solar sail	MG	MG	MP	MG	MP	F	0.47
Human rated inflated structure	F	G	F	MP	MP	P	0.45
Inflatable systems for re-entry vehicle	F	MG	F	MP	F	F	0.54
ISRU radiators	MG	F	MP	P	P	MP	0.16
ISRU crucibles	MG	MG	MP	MP	P	F	0.38

4.2 Sensors selection

The following sensors were identified as interesting for the DSA product:

- Sensors capable of tracking the relative attitude towards the Sun.
- Vibration sensors.
- Temperature sensors.
- Sensors of the flux in the UV spectrum.
- Sensors of the fluence of protons.

As the expertise of LIST is on strain and temperature sensors, we focused the literature review on existing Commercial off-the-shelf (COTS) and in-house technologies of LIST that could fulfil the requirements. These options have been compared to each other and to determine which of identified candidates were best suited, a trade study was performed. The results of the trade-off are presented to follow:

Table 5. Results of the trade-off study for the selection of the sensors to be embedded into the space product adopted within this activity.

Candidate	Compliance with the requirements	Integration process adaptability	Cost	Innovation potential	Structural influence on the product	Score
Commercial Thermistors	MG	MP	MP	P	P	0.28
Commercial Thermocouples	F	P	G	P	F	0.35
Commercial RTDs	MG	F	F	P	MP	0.38
Optical Fibre Bragg Gratings	F	P	P	P	F	0.24
Commercial Strain Gauges	MG	F	F	P	G	0.53
Inkjet-Printed RTDs	**F**	**G**	**MG**	**G**	**G**	**0.75**
Inkjet-Printed Strain Gauges	**F**	**G**	**MG**	**G**	**G**	**0.75**

4.3 Deployable Solar Array (DSA) design

The Deployable Solar Array (DSA) configuration was driven by mission requirements, aiming to produce 50W BOL and fit two DSAs within a 1U CubeSat. This design ensured that the spacecraft's center of gravity remained stable post-deployment. Due to the limitations of encapsulated flexible PV cells, a foldable configuration was chosen to utilize rigid PV cells effectively. Using Triple-junction Ga-As PV cells from Azur Space for LEO missions as a reference, a minimum of 47 cells was required to meet power needs. Additionally, the DSA was designed to deliver unregulated power with a voltage range at the maximum power point (Vmpp) from 13.8 to 24.0 V, aligning with standard CubeSat EPS requirements. The resulting preliminary design of the DSA is shown in Figure 2.

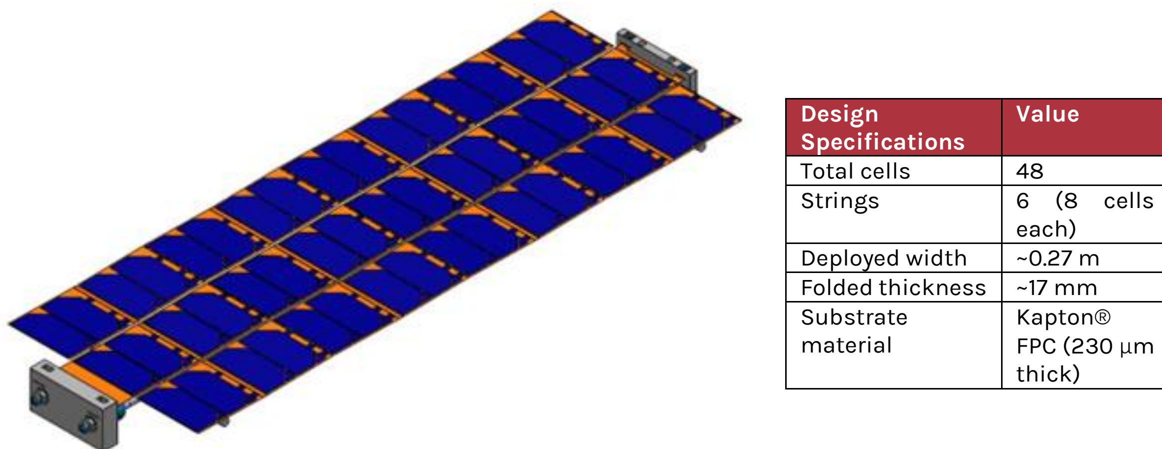

Design Specifications	Value
Total cells	48
Strings	6 (8 cells each)
Deployed width	~0.27 m
Folded thickness	~17 mm
Substrate material	Kapton® FPC (230 μm thick)

Figure 2. A DSA in its deployed configuration and summary of its specifications.

The DSA featured 48 cells arranged in six strings of eight, yielding a BOL Vmpp of ~19.3 V. Each cell had a bypass diode for failure tolerance against impact damage. To minimize extension from the CubeSat, the cells were arranged in three rows with two independent strings per row, reducing the maximum extension from 2.55 m to 0.87 m. The cells were mounted on a 230-µm-thick Kapton® flexible PCB (FPC), which enabled the DSA to fold in an accordion-like pattern. Each pair of PV cells formed a segment, as depicted in Figure 3 (left).

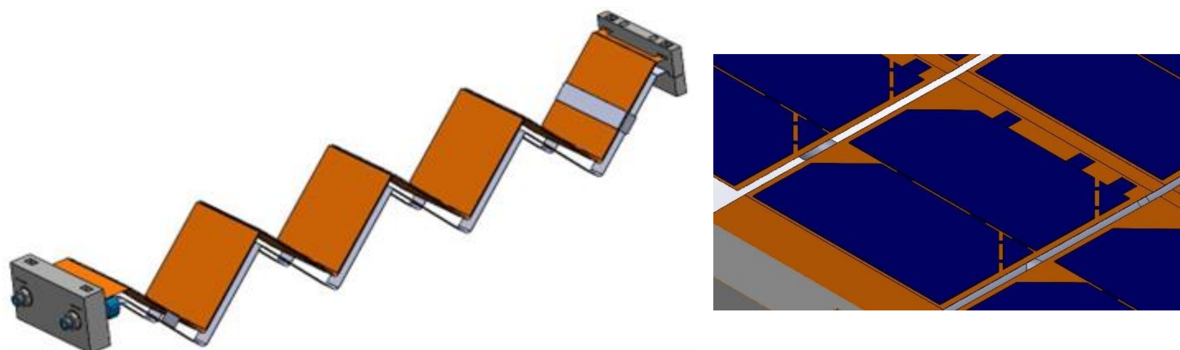

Figure 3. Left: a DSA with lateral rows folded on the central one. Right: highlight of the segmented structure of the DSA, where each pair of PV cells forms a rigid segment connected to other segments by FPC.

Each row's segments were connected via the FPC, serving as a flexible hinge. Cells were bonded using conductive silver epoxy for electrical contact or silicone adhesive for mechanical support. Silver-coated Kovar ribbons provided electrical connections, while silicone adhesive ensured mechanical bonding, avoiding soldering to reduce thermal stress.
In its stowed configuration, the lateral rows folded onto the central row, with the FPC hinges enabling folding. The total folded thickness was 17 mm, meeting the requirement for stowing two DSAs in a 1U volume.
Strain and temperature sensors, embedded on the FPC's backside using InkJet Printing (IJP) by MRT-LIST, were electrically connected to the FPC. Temperature sensors at segment centers provided average readings, while strain sensors near hinges monitored stowing and deployment strain.

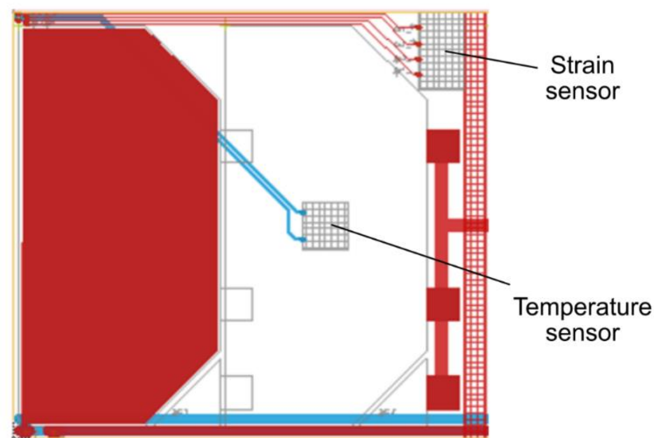

Figure 4. Diagram showing the position of the strain and temperature sensors on one segment of the DSA.

For deployment, Maana Electric proposed an inflatable system utilizing two flexible tubes positioned beneath the FPC of the central row. These tubes, once inflated, acted as rigid booms to deploy the central row. The deployment mechanism for the lateral rows remained under study, with options including an extension of the inflatable tubes in a branching configuration. The mechanical strength of sensors during deployment was evaluated through simulations to address potential damage from fast stretching during unfolding.

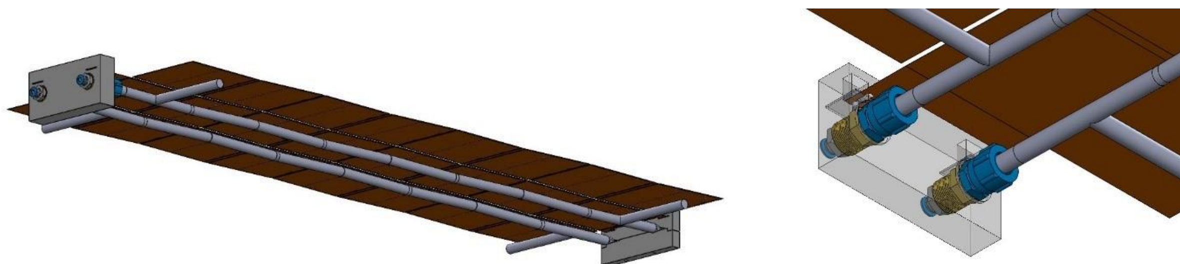

Figure 5. Left: the rear-side view of the deployed DSA, showing the deployable mechanism with proposed inflatable branching of the inflatable tubes. Right: highlight of the interface with the gas-management system and the physical holder of the Kapton® substrate.

4.4 Sensors manufacturing

During the activity, we analyzed and tested printed sensor manufacturing on different surface materials. The manufacturing process steps used for printing on substrates were:

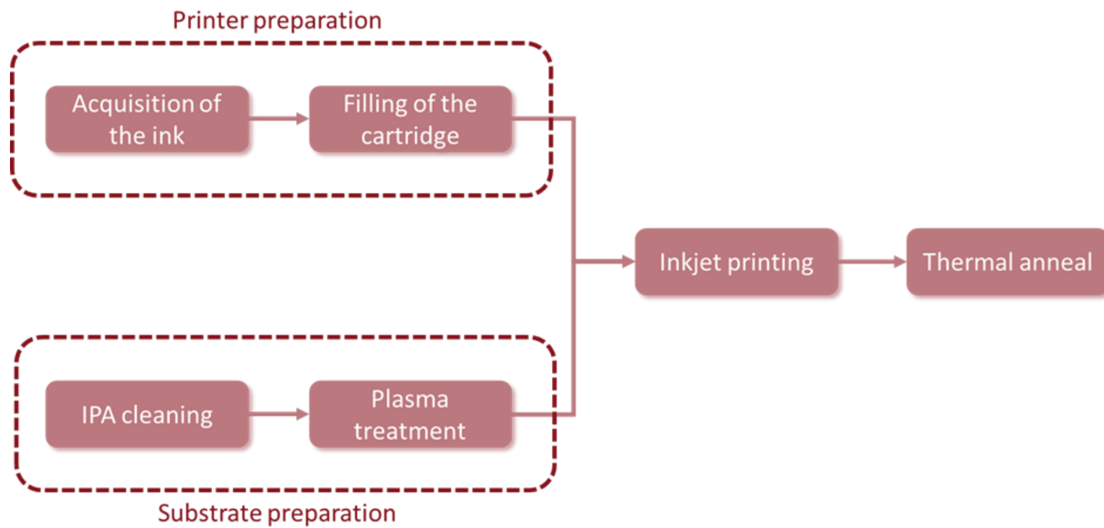

Figure 6. Process steps of sensors' inkjet printing proposed by LIST.

Two printing approaches were considered:

- In-situ printing: Sensors are printed directly onto the array structure without an additional substrate. This ensures inherent contact, a low profile, and seamless integration into the flexible panel manufacturing process but requires high material and process compatibility.
- Ex-situ printing: Sensors are printed separately on a substrate (e.g., Kapton®) and later attached. This approach simplifies process compatibility but requires an additional attachment step.

To embed sensors in the DSA's flexible PCB, a de-risking test campaign optimized the integration process. The ex-situ approach was chosen, with sensors printed separately and installed in dedicated slots within the flexible PCB, as shown in Figure 7.

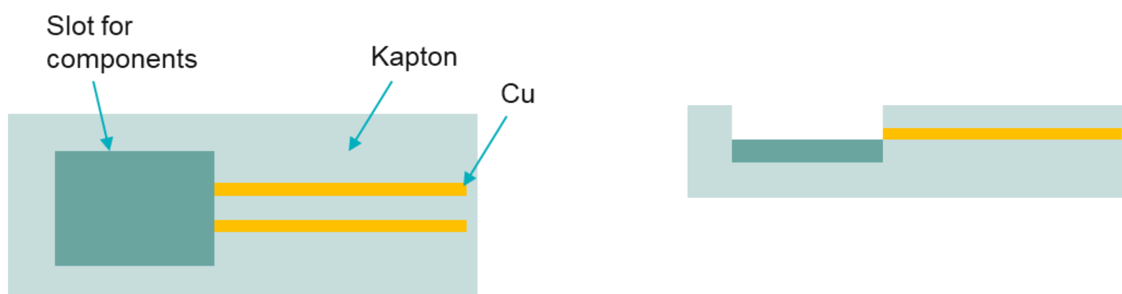

Figure 7. Top and side-view of the flexible PCB design for integration of printed sensors.

The flexible PCB consisted of embedded copper (Cu) conductors and a Kapton® substrate. Slots for different components (e.g., sensors) were created through an etching process performed by the PCB supplier. With this approach, the risk of mechanical failure due to fabrication was significantly reduced. The proposed process for integration of the gauges on such commercial substrates consisted of the following steps:

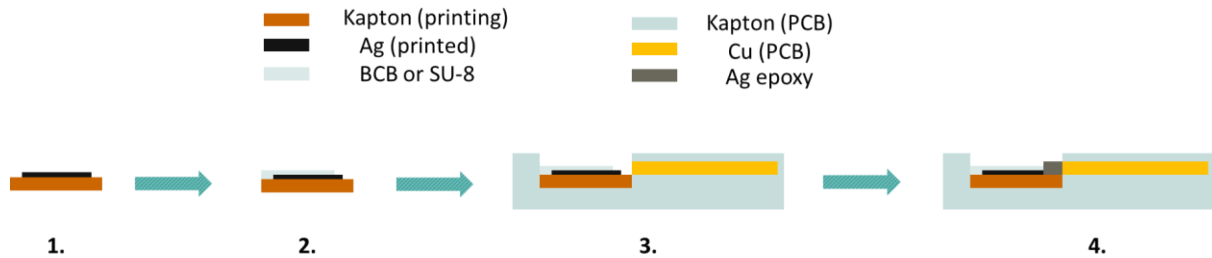

Figure 8. Proposed process flow for the manufacturing and integration of printed sensors into the DSA breadboards: 1) Printing of the gauge and the pads. 2) Spray-coating of an encapsulant. 3) Gluing sensors onto the flexible PCB. 4) Application of Ag epoxy.

4.4.1.1 Inkjet printed sensors' design

The final design of the inkjet printed sensors was the result of some optimization tests carried out on each gauge configuration.

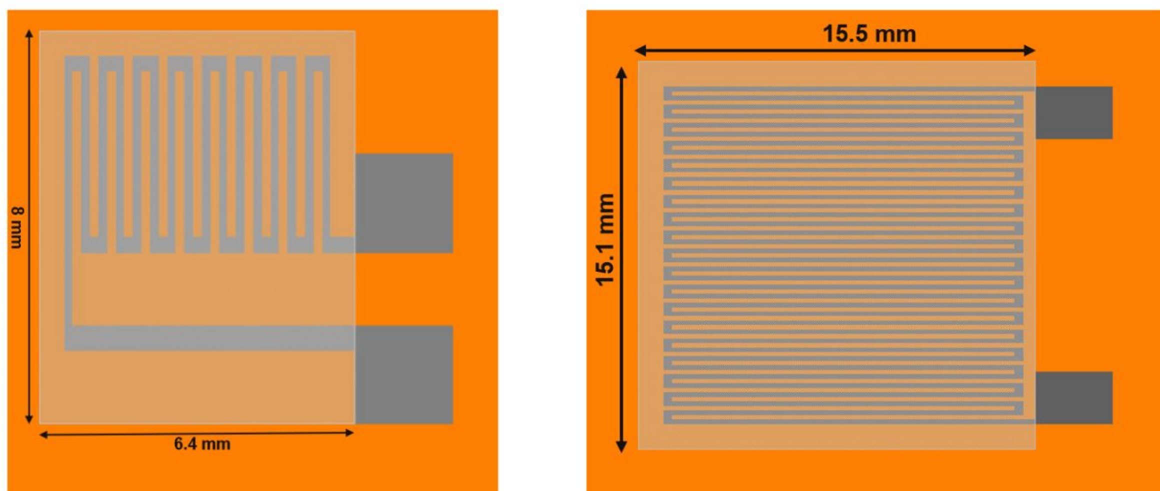

Figure 9. Final design of strain gauges and temperature sensors.

4.5 Breadboards

As a next step, we proposed a de-risking of the activity by developing some breadboards on which the sensors would have been embedded and tested in the relevant environmental conditions before implementing these in the actual design of the DSA. The relevant environment included effects that are testable at scaled-down

size (such as thermal vacuum) and others that require full-scale testing to be representative (such as for launch loads). This is especially true for testing the effect of deployment on the mechanical integrity of the embedded sensors and their physical connection. On the other hand, TVAC testing of an inflatable with the typical dimensions of the DSA was impractical in terms of budget and available facilities. For these reasons, we proposed to develop two independent breadboards to test the compatibility with relevant environment:

- DSA PV-representative breadboard (DSA-PV).
- DSA mechanical-representative breadboard (DSA-M).

4.5.1 DSA-PV

This breadboard was meant to demonstrate the compatibility of the product with embedded sensors against environmental conditions subject to scaling effects. It was therefore representative of the photovoltaic assembly, as well as of the configuration/placement of sensors and electrical connections.

4.5.1.1 Design

The DSA-PV was designed to be representative of a single string of the DSA. It was composed of a monolithic FPC, 230 µm thick, with eight PV cells integrated on top. The CAD representation of the DSA-PV is shown in Figure 10. The breadboard included four lateral extensions, which were secured (with appropriate tolerances) to the supporting structure via the pre-designed holes. It also featured a data and electrical interface that was strengthened with stiffeners, resulting in a total thickness of approximately 400 µm.

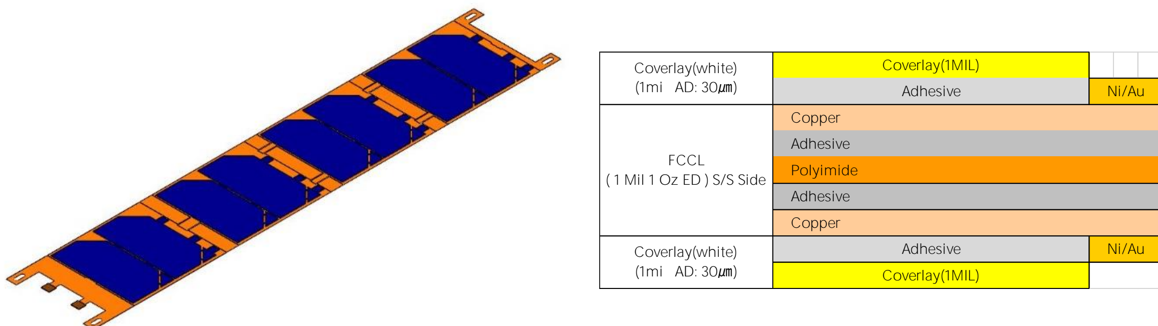

Figure 10. Left: CAD representation of the DSA-PV. Right: Stack structure of the FPC layers for the DSA breadboards.

The FPC structure, used in both DSA-PV and DSA-M (Figure 10), featured a two-layer copper stack for overlapping electrical and data lines without interference. It was protected by top and bottom coverlays and laminated with adhesive, with Ni/Au pads enabling connections between cells, sensors, and copper layers. PV cells were arranged into four segments, separated by 14 mm flexible joints. To prevent damage

to the laminated copper layers, a minimum bending radius of 2.3 mm was enforced, as FPCs require at least 10 times their thickness. To avoid accidental over-bending (e.g., during AIT activities), connections were embedded in bridges designed for larger radii. A CAD representation (Figure 11) illustrates the folded DSA-PV and connection bridges. Their placement was alternated along segments to prevent interference during bending. Bridges were pre-cut during manufacturing with rounded corners to reduce mechanical fatigue and cracking.

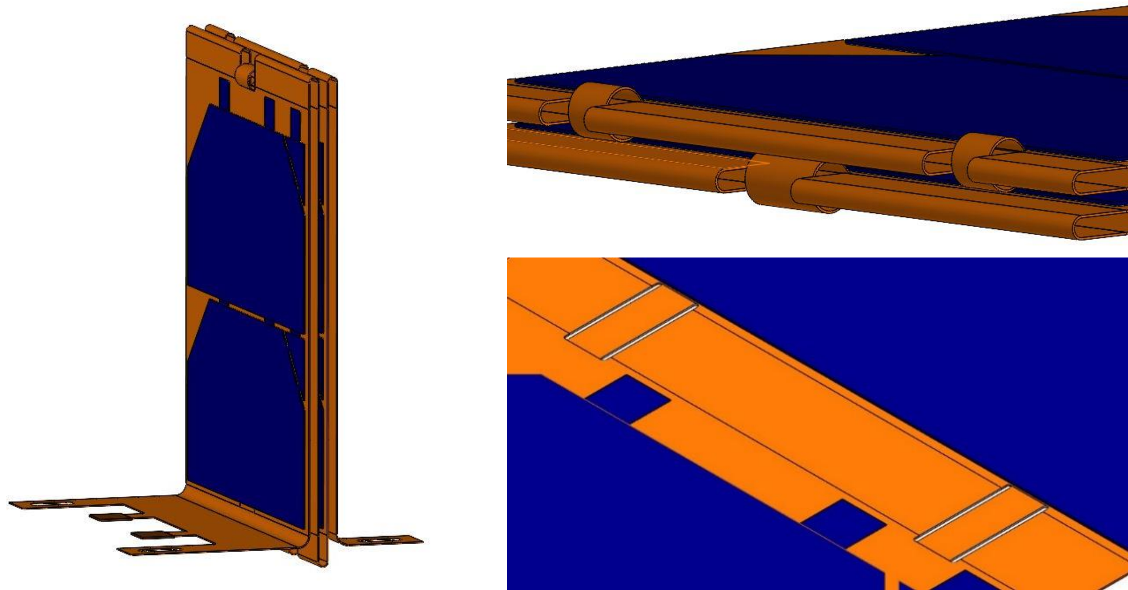

Figure 11. Right: CAD of the folded DSA-PV. Left: Highlight of the connection bridges when the segments were folded (top) and in the deployed configuration (bottom).

The PV cells were electrically connected to the FPC using conductive silver epoxy with bond lines as thin as 100 µm. In each segment, the first PV cell's rear surface was connected to the FPC via a circular tab of silver epoxy, while uncovered areas were bonded with silicone adhesive. The first cell's interconnects linked to the rear of the second cell, which was then connected to four small FPC pads via silver epoxy. Electrical connections between segments were routed through the connection bridges, which also included sensor wiring. Where no electrical connection was needed, the second PV cell in each segment was attached with insulating silicone adhesive. Figure 12 illustrates the electrical circuit, with thick lines representing the top and bottom FPC layers. As per requirements, the DSA-PV breadboard included two sensors of each type, with one temperature sensor and two strain sensors embedded every two segments. Using two strain sensors enabled the separation of temperature-induced strain from mechanical strain. Their positions and wiring layout are shown at the bottom of Figure 12.

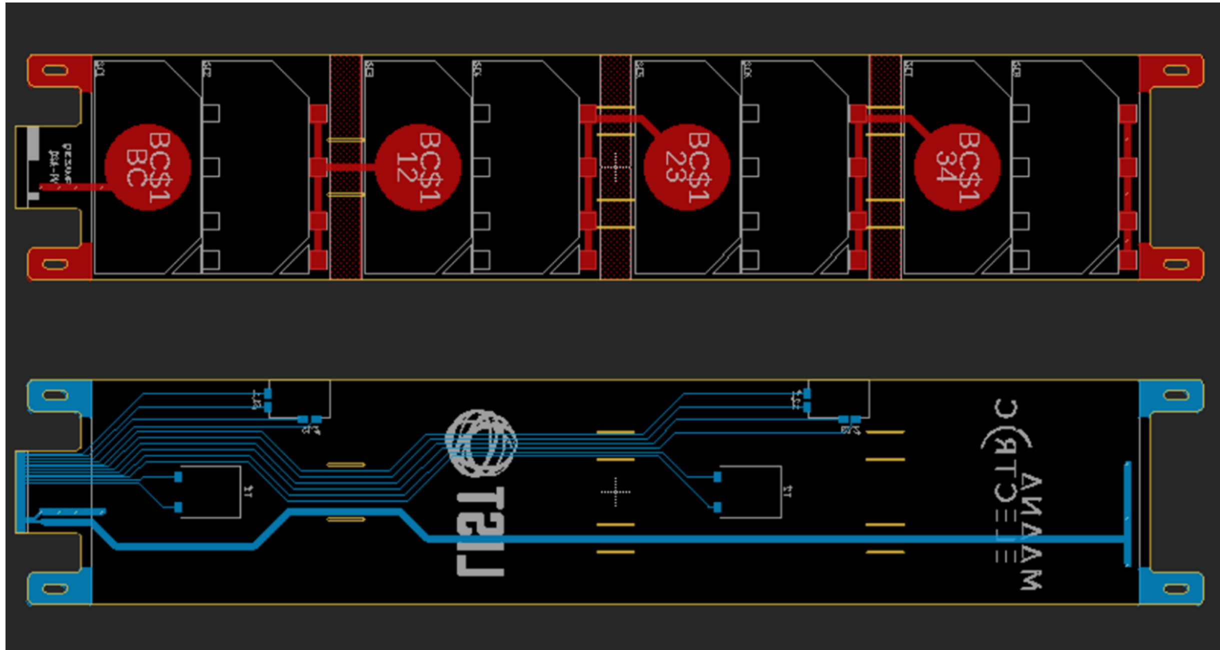

Figure 12. Electrical and data design of DSA-PV's FPC. The top layer of the embedded circuits embedded in the PCB is on top of the Figure and highlights the circular pads for rear-connection of the first cells of a segment, the small square pads for connection of tab-wires of the second cells of a segment and finally the electrical connection between electrical interface and first segment, as well as electrical connections between segments. The bottom of the Figures shows the embedded circuits on the bottom layer of the FPC, which includes the electrical connection between the last segment and the interface (return electrical line), as well as the four sockets for the sensors and their data connections to the data interface.

4.5.1.2 TVAC testing

TVAC testing on the DSA-PV was performed at external service provider Lunar Outpost EU (Luxembourg). Their vacuum chamber allowed testing at ultimate vacuum below $5x10^{-6}$ mbar. The temperature of the thermal plate was controlled by recirculating silicone oil. The temperature of the shroud was not controlled. The DS-PV integrated on a specially designed thermal plate is shown in Figure 13a. 0.5 mm thick thermal filler made of SigraFlex® (Figure 13b) was placed between the two thermal plates to enable good thermal contact. To enable live measurements, the cables were connected through the KF50 feedthrough.

(a)

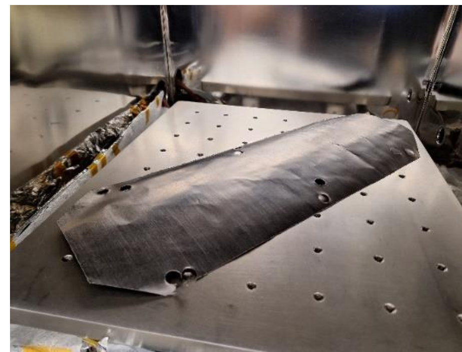

(b)

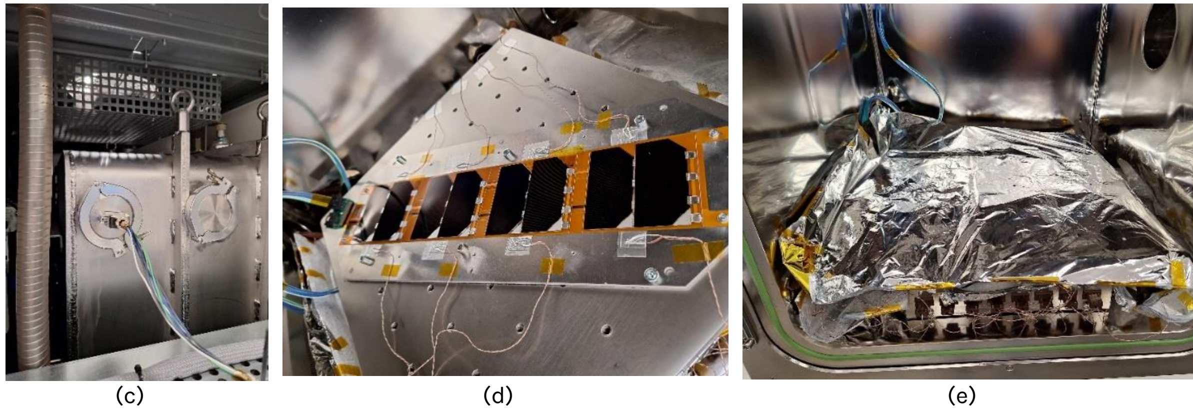

Figure 13. TVAC set-up with the DSA-PV demonstrator. a) The demonstrator integrated on a thermal plate. b) Thermal filler (Sigraflex® graphize foil) which was placed between the two thermal plates. c) Flange with the KF50 feedthrough. d) The demonstrator integrated on thermal plate with attached thermocouples. e) The whole set-up is covered with MLI.

Reading of the temperature and strain sensors is shown in Figure 14. Both temperature sensors followed well the temperature profile with practically no resistance value drift. It is important to note that the resistance value at RT was very close to those measured after sensor integration. Both strain sensors behaved similarly and followed closely profile of the temperature change.

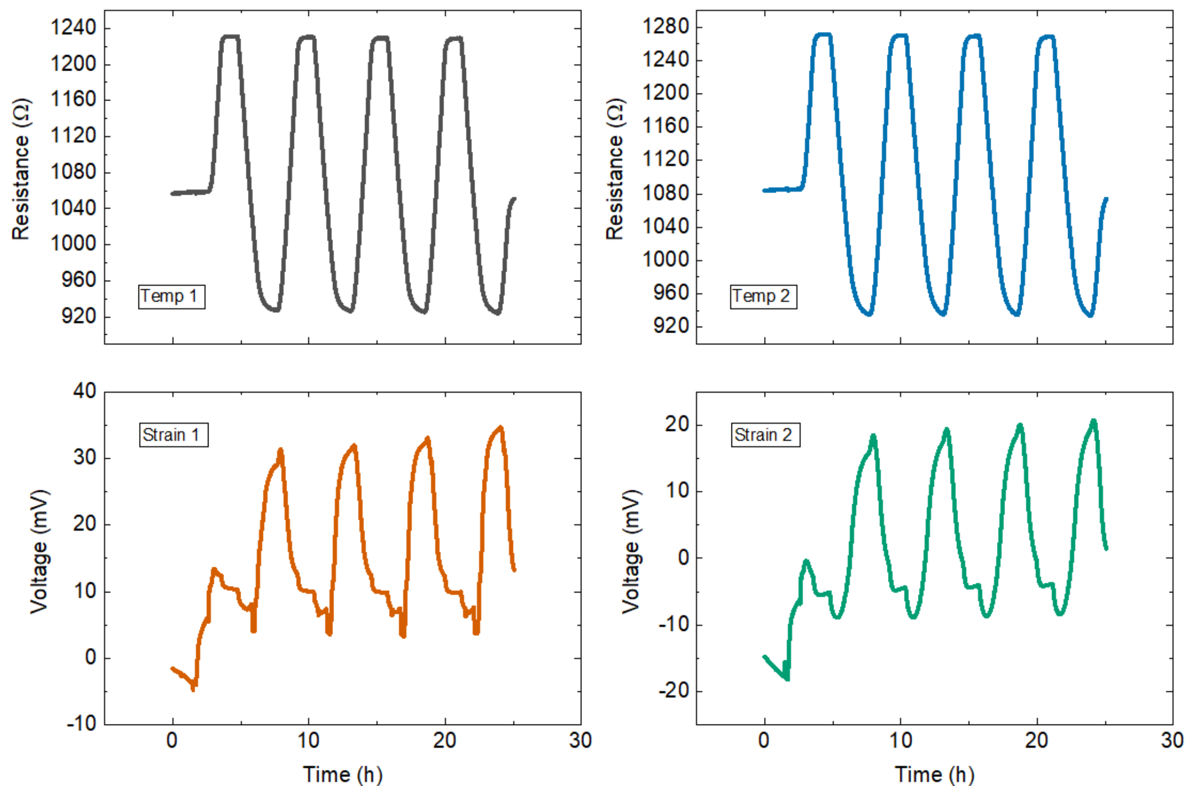

Figure 14. Response of the sensors integrated on the DSA-PV during TVAC cycling experiment.

In addition, visual inspection of the DSA-PV after the TVAC experiment showed no changes w.r.t. to the state before the test were observed (see Figure 15).

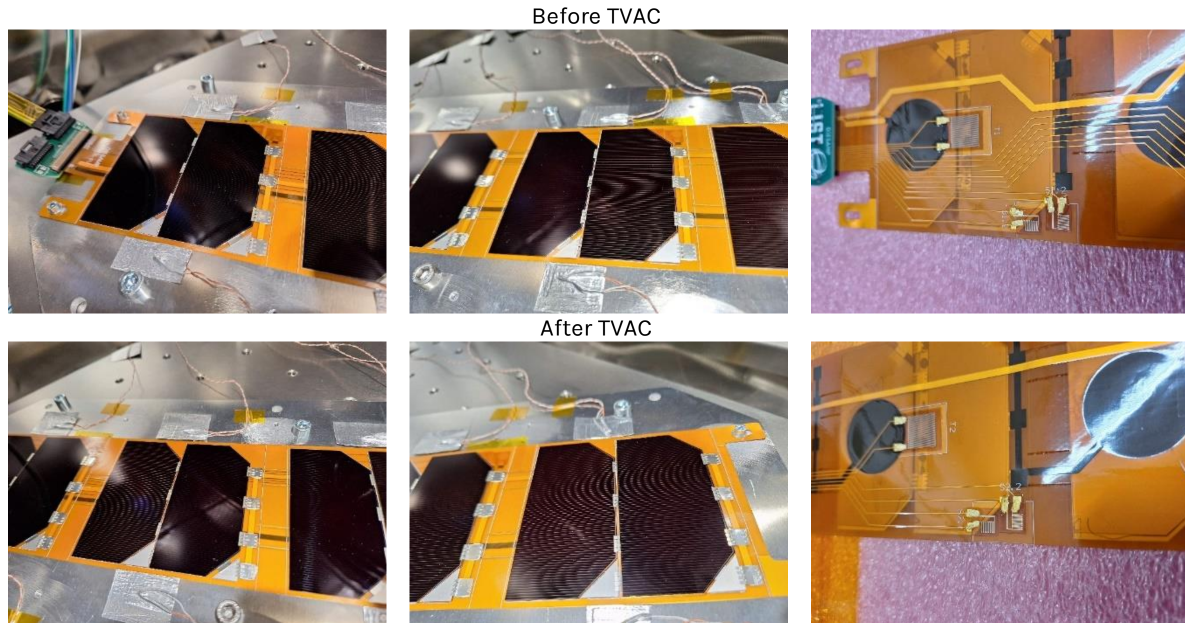

Figure 15. Visual appearance of the DSA-PV demonstrator before and after TVAC tests.

Results of the TVAC tests are summarized in the following Table comparing the pass/fail criteria.

Table 6. Summary of the results of TVAC testing on the DSA-PV breadboard.

DSA-PV Thermal Tests	
Pass/Fail criteria	Status after testing
The breadboard passed a Physical Inspection, PV Functional and Sensors Functional tests before testing.	All the tests performed, results positive.
The temperature profile is followed with respect to set temperature, TRP and dwell time.	Temperature profiles according to the test plan. Slight deviation of pressure (~10^{-4} mbar instead of 10^{-5} mbar) during TVAC hot and TVAC cold is considered a minor deviation.
The sensors function with required performance and accuracy during the test.	Real-time data taken during testing revealed expected behavior. Drift of the resistance values was observed during TVAC hot in one of the temperature sensors, while it was very minor in the others, which confirms improved behavior of the new encapsulation (additional SU8 layer and additional PU140 layer). However, as one of the sensors still showed strong drift the encapsulation (or its process) can be further improved.
The breadboard passed a Physical Inspection, PV Functional and Sensors Functional tests after testing.	All tests were successfully performed.
The performance of the sensors is the same of those recorded before the TVAC testing, within uncertainty of precision.	Temperature and strain sensors give very similar resistance and voltage reading before and after the tests. The exception is one of the temperature

	sensors, which shows a resistance drift during first TVAC hot test.

4.5.2 DSA-M

This breadboard was meant to demonstrate the compatibility of the embedded sensors to the relevant mechanical environment and during operations. It was therefore representative of the full-scale mechanical design of the DSA in its longitudinal deployment.

4.5.2.1 Design

The DSA-M was designed to be representative of an entire row of the DSA. It was composed of two strings of eight cells each: four PV cells and four mechanical cells. The mechanical cells provided the correct mechanical response without containing a functional photovoltaic stack. This approach is commonly used in low-TRL activities to focus on the mechanical response of a breadboard, enabling a representative simulation of the actual product while remaining compatible with the project's budget constraints. The CAD representation of the DSA-M is shown in Figure 16, where PV cells and mechanical cells are depicted in blue and dark grey, respectively.

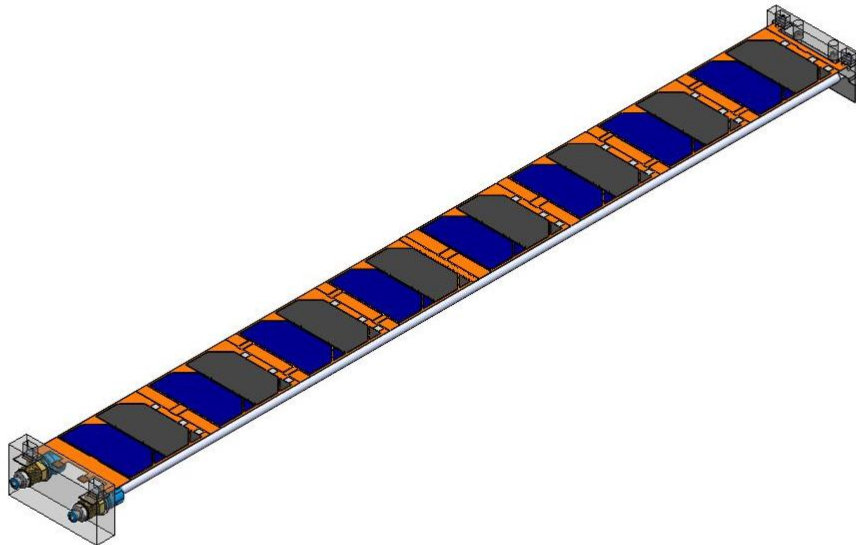

Figure 16. CAD representation of the DSA-M.

The second cell in each segment was mechanical and was therefore not electrically connected to the FPC. To preserve the electrical connection between segments of the same string, the first cells of every segment shall be connected from both rear and from connections to the electrical circuits. As in DSA-PV, circular pads were used for the rear electrical connection of the first cells via silver epoxy. Thea area not covered by epoxy was mechanically attached to the FPC through silicon adhesive. The small square pads for the cell's front connection were shifted in the middle of the segment, so that it was possible to bond the tabs of the first cell directly to the electrical circuit on the top layer of the PCB. The mechanical cell was bonded to the FPC using silicone

adhesive. The electrical lines are shown as thick red and blue lines in Figure 17. Contrary to the electrical design of the DSA-PV, the onward and backward electrical lines of both strings were routed on both top and bottom layers of the FPC to avoid superposition with other lines.

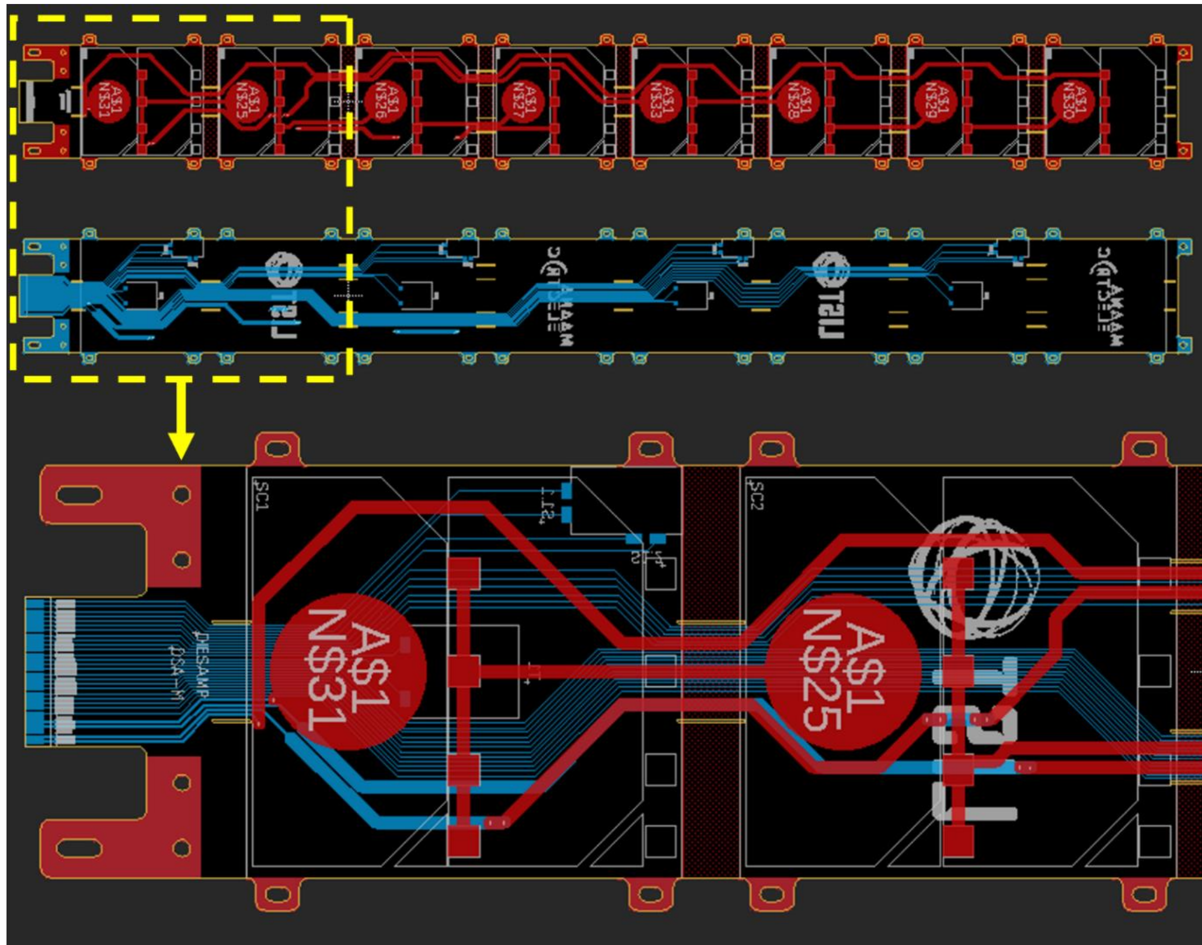

Figure 17. Electrical and data design of DSA-PV's FPC. The top and bottom layers of the FPC are shown at top of the Figure. Details of the circuits in the two overlapping layers of the first two segments are shown at the bottom of the Figure.

Electrical lines were distributed across both FPC layers, while data lines were placed only on the bottom layer to avoid resistance variations from layer shifts. Data connections in DSA-M are shown as thin blue lines in Figure 17. The breadboard, scaled to match the number of sensors per DSA row, included four pairs of strain sensors and four temperature sensors, with sensor positions marked by embedding sockets in Figure 17.

The DSA-M also featured a deployment system representative of the inflatable piping used in the DSA. Only the two main inflatable masts were implemented (Figure 18). Tubes were secured to holding blocks, with the root block attaching the tube to a threaded interface, where it was heated and compressed for adherence. Pneumatic sealing was achieved via a rubber-ringed dice, while the tube's tip was sealed through thermal pressing and secured to the tip holding block. These blocks also fixed the

FPCs with screws, ensuring proper alignment between the inflated tube's length and the FPCs.

Figure 18. Bottom view of the DSA-M in deployed configuration, showing the inflated tubes and their interfaces with the FPCs and the gas system.

4.5.2.2 DSA deployment testing

For deployment functional tests, a suspension system is used to reduce gravity effects in the direction of the deployment. The setup employed is shown in the following Figure. The gas system was interfacing a compressed air line.

Figure 19. Setup of deployment test: the DSA-M mounted in stowed configuration (top-left), a highlight of the data interface of the DSA-M (bottom-left), the DSA-M released from stowed configuration (top-right) and the DSA-M deployed with inflation.

During this test the response of the strain sensors during the “pressed”, “released”, and “inflated” stages of the deployment. The response is shown in Figure 20.

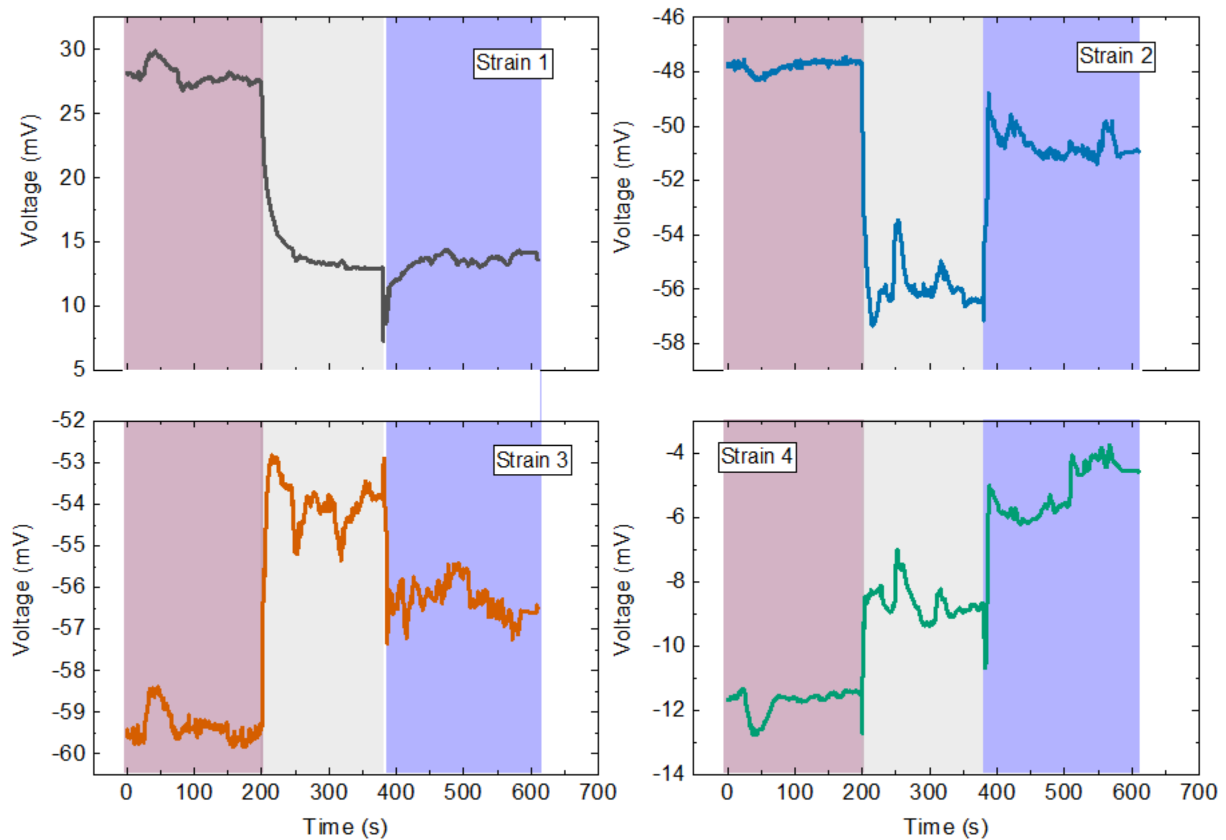

Figure 20. Strain sensors reading during deployment test. Different colors denote different stages of deployment: “pressed”, “released” and “inflated”.

For the case of strain 2, strain 3 and strain 4 sensors, there was a clear distinction between the three stages. For strain 1, the distinction between “released” and “inflated” stages was less clear, but still detectable. The reason for this (and different signatures for different stages observed in the other sensor) was in their different placement on the demonstrator. They experienced different strains, in addition, they were placed just below the inflatable tubes, which could further distort the reading. Despite these points to be improved, the test was considered successful.

Results of the tests are summarized in the following Table comparing the pass/fail criteria.

Table 7. Summary of the results of deployment testing on the DSA-M breadboard.

DSA-M deployment functional	
Pass/Fail criteria	Status after testing
The temperature sensors deliver information about the baseline environment.	Temperature sensors acquisition successful.
The sensors can read with required accuracy the value of the baseline environment.	Temperature sensors showed only minor drift of the resistance values. TCR can be used to calculated the temperature.

The strain sensors can uniquely identify folded vs. stowed configurations.	As shown in Figure 20, the sensors are able to distinguish "pressed", "released" and "inflated" stages of the deployment test.
Check-out inspection and tests do not highlight any difference in the sensors' status before and after execution of the Functional test.	Inspection successful.
Check-out inspection does not highlight any degradation of the PV assembly, of the FPC and inflation mechanism.	Inspection successful. Pre-existing damage on cells did not propagate. Comparison between pre- and post-test PV functional confirms that the deployment did not degrade the performance of the panel. The power measured is consistent within measurement error due to setup of the array within the Light-Box.

4.5.2.3 Sine loads and random vibrations

The setup for sine and random vibrations tests consists of the DSA-M integrated on the mechanical interface of a shaker available at the Technical University of Munich. An accelerometer is installed onto the interface between the CFRP structure and the array, on a plane normal to the direction of motion. The sensors are monitored through cables suspended on the setup to not alter frequency response. An image of the setup employed is shown in the following Figure.

Figure 21. Setup of x-axis vibratory test of DSA-M. Left: the mechanical interface. Center: the DSA-M mounted. Right: the accelerometer.

The test was performed according to the test specifications, except for the fact that it was not possible to perform the test at nominal acceleration level, due to some issues with the shaker. The test was performed with spectrum as by specifications (Falcon 9 spectrum) but with intensity at -3dB. This deviation was accepted, as the environment was sufficiently accurate to have first indications of resistance of the sensors to the environment.

Readings of the strain and temperature sensors during random vibration tests on x-axis, y-axis and z-axis test are shown in Figure 22, Figure 23 and Figure 24 respectively. The grey area highlights when the random vibration tests were executed. Both strain sensors #3 and #4 identified the vibratory environment in both x and z directions. Instead, strain sensor #2 identified the environment for test in x direction,

while sensor #1 was not able to distinguish the environment from static reading. It must also be remarked that no sensor could identify vibrations in y direction. Regardless, as the actual random vibrations environment consisted of a superposition of the three axes, the sensors are expected to be able to identify a nominal vibratory environment during launch. The sensors demonstrated critical performance in a relevant launch environment, confirming their suitability for use during this mission phase to compare the nominal, expected conditions with potential anomalies arising from incorrect system integration on the launcher or other contingency scenarios.

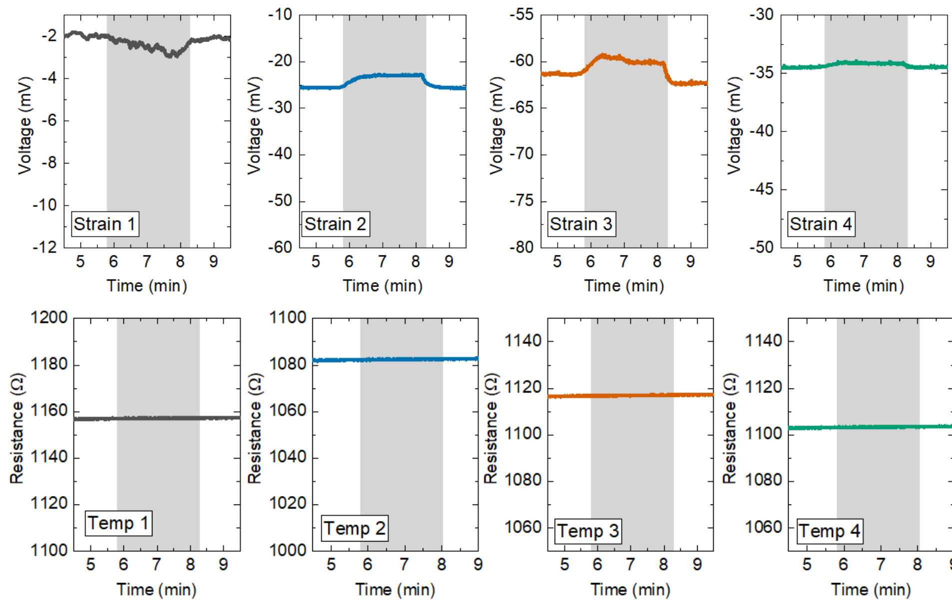

Figure 22. Readings of the strain sensors (top) and temperature sensors (bottom) during random vibrations test on the x-axis. Grey area highlights the time of interest for the shaker test.

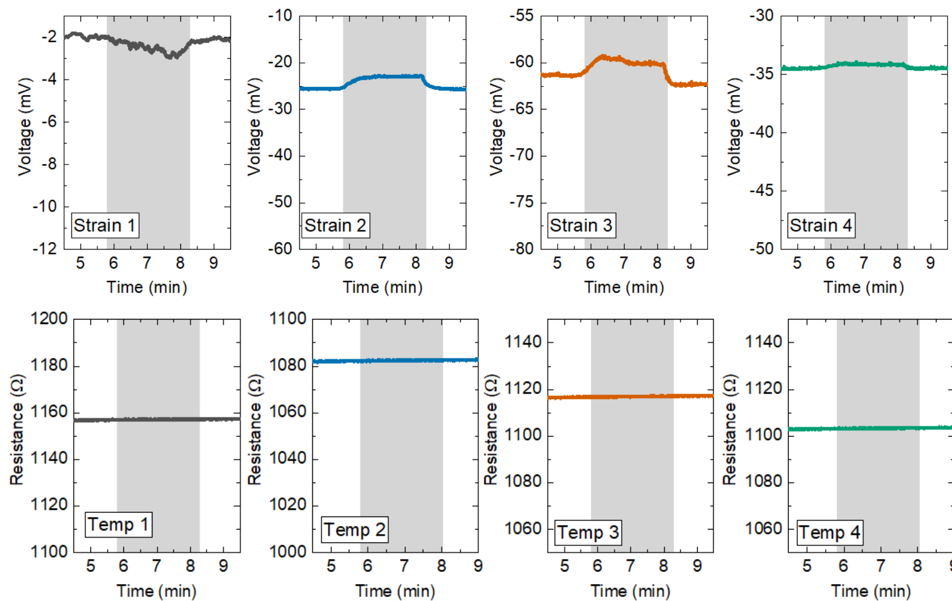

Figure 23. Readings of the strain sensors (top) and temperature sensors (bottom) during random vibrations test on the y-axis. Grey area highlights the time of interest for the shaker test.

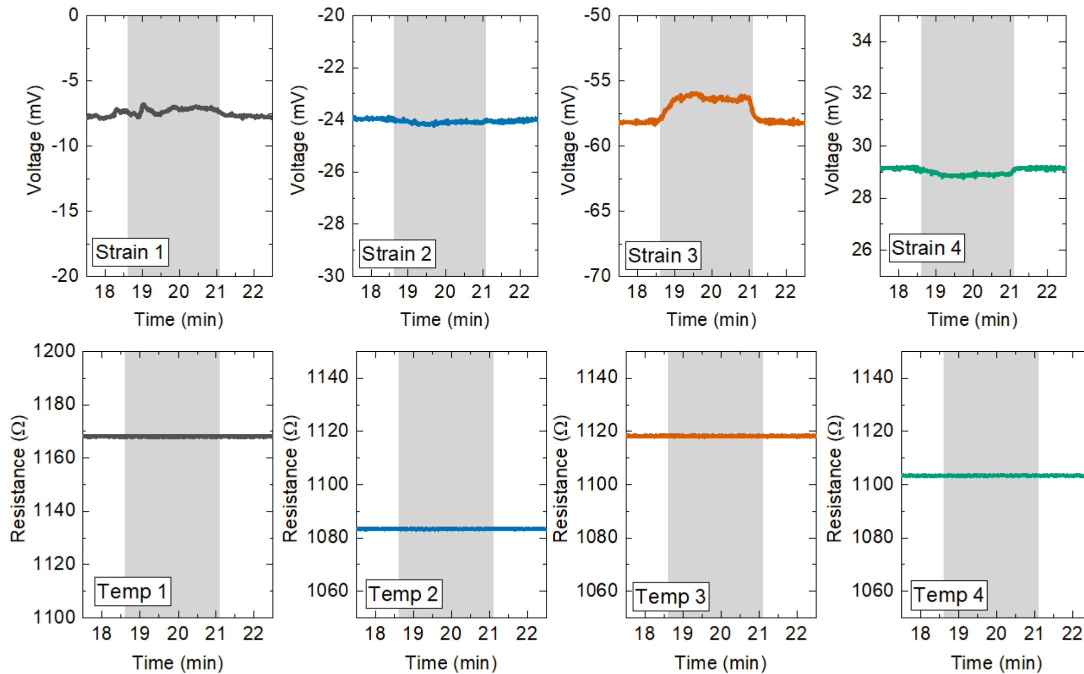

Figure 24. Readings of the strain sensors (top) and temperature sensors (bottom) during random vibrations test on the z-axis. Grey area highlights the time of interest for the shaker test.

Results of the tests are summarized in the following Table comparing the pass/fail criteria.

Table 8. Summary of the results of deployment testing on the DSA-M breadboard.

DSA-M Sine Loads and Random vibrations	
Pass/Fail criteria	Status after testing
The temperature sensors deliver information about the baseline environment.	Temperature sensors acquisition successful.
The sensors can read with required accuracy the value of the baseline environment.	There is no influence of the vibration environment on the temperature-sensor reading.
The strain sensors can uniquely identify the vibratory environment vs. static folded or stowed configurations.	Monitoring the strain sensors is possible to uniquely identify a vibratory from a static environment. Readings of embedded strain sensors during random vibration tests are shown in Figure 22, Figure 23 and Figure 24.
Check-out inspection and tests do not highlight any difference in the sensors' status before and after execution of the Functional test.	Visual inspection successful.
Check-out inspection does not highlight any degradation of the PV assembly, of the FPC and inflation mechanism.	Visual inspection successful. Pre-existing cracks did not propagate during the test. The sine tests performed before and after each random vibration test are congruent for all three axes.

As part of the check-out inspection, PV functional and Deployment functional tests were performed. Results of PV functional test showed no degradation of photovoltaic performance during and after test execution.

5 Conclusions and future developments

The DIESAMP project aimed to demonstrate the feasibility of integrating advanced manufacturing techniques with embedded sensor technologies into space products in order to take advantage from real-time monitoring and operational reliability across diverse phases of the product life cycle. In the frame of a survey, it was decided to adopt as a reference space product a novel concept of Deployable Solar Array developed by Maana Electric based on the concept of flexible PCBs. In this framework, inkjet printed temperature and strain sensors developed by the Luxembourg Institute of Science and Technology have been embedded.

Breadboards of the DSA with embedded sensors have been developed and manufactured, successfully demonstrating the feasibility of integrating the sensors into the DSA design. By embedding strain and temperature sensors into flexible printed circuit boards (PCBs), the project validated key processes and achieved a Technology Readiness Level (TRL) of 4 through rigorous testing in relevant environmental conditions.

The testing campaign confirmed the robustness of the embedded sensors and manufacturing processes, showcasing their ability to withstand harsh space conditions while maintaining critical performance. However, it also highlighted areas for refinement, both for the sensors manufacturing process and the DSA design. In particular:

- Resistance drift experienced in printed sensors necessitates improvements in encapsulation materials and deposition processes to ensure consistent sensor performance.
- Observations of photovoltaic cell damage during integration and handling phases emphasized the need to adopt thin and flexible solar cells in place of the traditional rigid solar cells, which goes in the direction of design solutions considering for increasing power-to-mass ratio of new space solar array configurations.

Building on the insights gained, the project has outlined a clear roadmap for advancing this technology. Near-term efforts shall focus on addressing identified challenges, scaling production through innovative techniques like aerosol jet printing, and transitioning the technology toward higher maturity levels. The mini-FLEX solar array, conceived as an evolution of the DSA concept developed under this activity, represents a first step towards commercialization targeting CubeSat applications, paving the way for subsequent iterations having the ultimate goal in implementing the technology for lunar exploration and advanced satellite missions.